

Courtney Johnson¹, Augustino Scorzo¹, Gaspare Carollo¹, Nakoa Webber², Alex Calabrese¹, Aubrie A. Weyhmiller¹, Taylor V. Douglas¹, Kayla A. Callaway¹, Nathaniel V. Nucci^{1,2}

¹Dept. of Physics and Astronomy, ²Dept. of Molecular & Cellular Biosciences
Rowan University, Glassboro, NJ, 08028

Background

Quantum dots (QDs) are nanoscale semiconductor crystals with optoelectronic properties that have a variety of applications. The optoelectronic properties of quantum dots are closely related to their size. Therefore, the fabrication method of quantum dots is crucial in producing dots with specific properties.

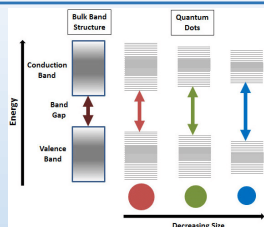


Figure 1: Size-tunable emission spectra of quantum dots [1]

Using reverse micelles (RMs) to control quantum dot crystal formation has the potential to offer a cost-effective, reproducible, and most importantly, scalable method for quantum dot fabrication. RMs are spontaneously-organizing nanobubbles of water surrounded by surfactant in a nonpolar solvent. RM size is controlled through water loading (molar ratio of surfactant to water)

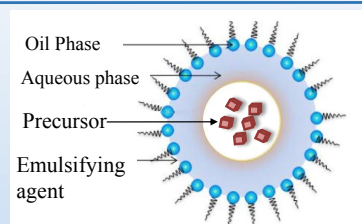


Figure 2: Reverse Micelle with cargo [2]

RM Exchange and the Population Balance Model

QD growth occurs through inelastic collisions and exchange between RMs.

The population balance model [4] describes nonparticle growth accounting for

- Intermicellar exchange rate (k_{ex})
- Distribution of particles ($p_{i,j}$)
- Probability of coagulation (k_{co})

Population balance equations:

$$\frac{dp_{i,j}}{dt} = k_{ex} C_m p_{i,0} p_{j,0} - k_{ex} C_m p_{i,j} p_{0,0} - k_{co}(i,j) p_{i,j}$$

$$\frac{dp_{0,0}}{dt} = \frac{1}{2} k_{ex} C_m \sum_{i=1}^{\infty} \sum_{j=1}^{\infty} p_{i,0} p_{j,0} - k_{ex} C_m \sum_{i=1}^{\infty} \sum_{j=1}^{\infty} p_{i,j} p_{0,0}$$

$$\frac{dp_{i,0}}{dt} = k_{ex} C_m \sum_{j=1}^{\infty} p_{i,j} p_{0,0} - k_{ex} C_m \sum_{j=1}^{\infty} p_{i,0} p_{j,0} + \sum_{k=1}^{i/2} k_{co}(i-k, k) p_{i-k, k}$$

where $k_{co} = C_1 \exp(-C_2 \frac{2d_{p1} d_{p2}}{d_{p1} + d_{p2}})$

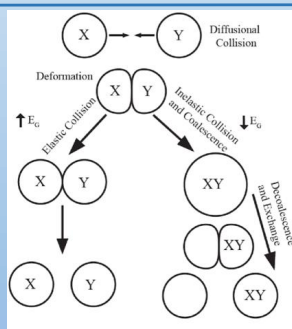


Figure 3: RM collisions and exchange [3]

Based on this model, variables to be tested were chosen:

- Viscosity of organic
- Time
- Water loading (W_0)
- Precursor Amount

Trend Analysis

The locations and intensity counts of the seed and quantum dot peaks were extracted from the EEMS data using a MATLAB script, then compiled with W_0 , viscosity of organic, and time point to run a data mining statistical analysis in R.

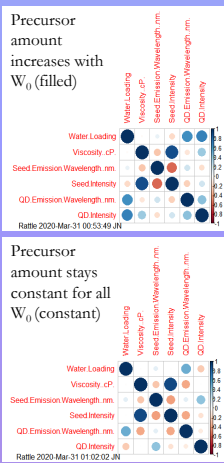


Figure 6: Correlation table from trend analysis

Water loading: strong (+) correlation between W_0 and QD emission wavelength; reflects literature

Viscosity: very strong (+) correlation between seed intensity and viscosity as well as (-) correlation between QD emission wavelength and viscosity; agrees with expectation that higher viscosity reduces yield of mature QDs due to less inelastic collisions between RMs

Precursor Amount: strong (+) correlation between QD intensity and W_0 in filled series while constant series shows (-) correlation; there is less precursor in the constant system to form the larger QDs as W_0 increases, resulting in a lower yield. Therefore, QD yield can be controlled through amount of precursor in the system.

Excitation-Emission Spectra

Fluorescence data was gathered in the form of excitation-emission spectra. These spectra consist of two signals: seeds (from nucleation) and mature quantum dots. EEMS was taken daily for four days, allowing for the growth of the QDs to be observed.

An example series of EEMS spectra is shown in Figure 5. This set allows Ostwald ripening (seeds dissolve and redeposit on larger crystals to form mature QDs) to be observed. Day 0 shows a high intensity of seeds that decreases through Day 3, where there is a higher intensity of QDs.

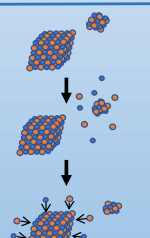


Figure 4: Ostwald Ripening process of crystal growth

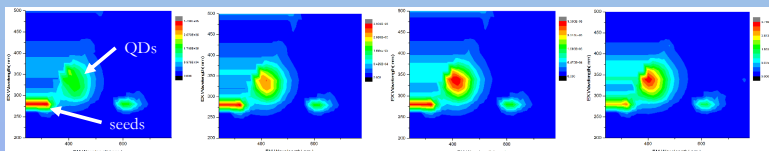


Figure 5: EEMS spectra for filled heptane sample of water loading 4 for Day 0 (left) through Day 3 (right).

EEMS to Size Distributions

In order to apply the population balance model to analyze the data, the EEMS spectra must be converted to size distributions. The Nosaka model for particle size vs. excitation energy was used [5]

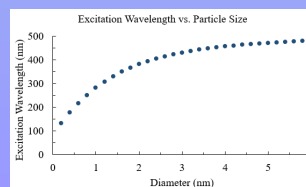


Figure 7: Reproduced graph of Nosaka model

The intensities for each excitation wavelength (200-500 nm) for the location of the QD peak were normalized and used as the frequencies for the corresponding particle sizes.

$$E_{ex} = E^{BPP} + V_0 \left(a_1 + \frac{b_1}{(R\sqrt{V_0 m_e^*/m_e} + c_1)^2} + a_2 + \frac{b_2}{(R\sqrt{V_0 m_h^*/m_e} + c_2)^2} \right) - \frac{1.8e^2}{\epsilon R}$$

R is radius of the particle, m_e^* and m_h^* are effective mass of the electron and hole respectively, ϵ is permittivity of CdS, c is charge of the electron, E^{BPP} is band gap energy, V_0 is finite potential well depth, and E_{ex} is excitation energy

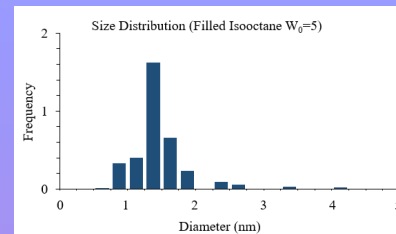


Figure 8: Example size distribution histogram for filled isoctane sample of water loading 5

Next Steps

- Convert all EEMS spectra to size distributions
- Apply population balance model to further analyze data

Acknowledgements

The authors would like to thank the New Jersey Health Foundation and the NASA New Jersey Space Grant Consortium for supporting and funding this research project.

References

- [1] Sigma-Aldrich: "Quantum Dots," <http://www.sigmaaldrich.com/materials-science/nanomaterials/quantum-dots.html> (accessed on 28 February 2019).
- [2] Qadir, A., Faiyazuddin, M., Hussain, M. T., Alshammari, T. M., & Shaked, F. (2016). Critical steps and energetics involved in a successful development of a stable nanoemulsion" *Journal of Molecular Liquids*, 214, 7-18. doi:10.1016/j.molliq.2015.11.050
- [3] Fletcher, P. D. I., Howet, A. M., Robinson, B. H. & H. K. C. T. N. The Kinetics of Solubilize Exchange between Water Droplets of a Water-in-Oil Microemulsion. 985-1006 (1987).
- [4] Sato, H. Asaji, N., & Komasaava, I. (2000). A population balance approach for particle coagulation in reverse micelles, 39(2), 328-334. doi:10.1021/ie990523j
- [5] Nosaka, Y. (1991). Finite Depth Spherical Well Model for Excited States of Ultrasmall Semiconductor Particles. An Application. *J. Phys. Chem.*, 95(13), 5054-5058.